



## Open Archive TOULOUSE Archive Ouverte (OATAO)

OATAO is an open access repository that collects the work of Toulouse researchers and makes it freely available over the web where possible.

This is an author-deposited version published in : <http://oatao.univ-toulouse.fr/>  
Eprints ID : 20170

**To link to this article :**

URL <http://www.ijer.irponline.in/>

**To cite this version :** Romdhane, Hela, and Soualmia, Amel, and Cassan, Ludovic, and Masbernat, Lucien *Evolution of flow velocities in a rectangular channel with homogeneous bed roughness*. (2017), International Journal of Engineering Research vol. 6, n° 3, pp. 120-125

Any correspondence concerning this service should be sent to the repository administrator: [staff-oatao@listes-diff.inp-toulouse.fr](mailto:staff-oatao@listes-diff.inp-toulouse.fr)

# Evolution of Flow Velocities in a Rectangular Channel with Homogeneous Bed Roughness

Hela Romdhane<sup>1</sup>, Amel Soualmia<sup>1</sup>, Ludovic Cassan<sup>2</sup>, Lucien Masbernat<sup>2</sup>

<sup>1</sup>Laboratory of Water Sciences and Technology, National Institute of Agronomy of Tunisia, University of Carthage, Tunis, Tunisia

<sup>2</sup> Fluid Mechanics Institute of Toulouse, INP Toulouse, University of Toulouse, Toulouse, France  
Corresponding Email: amel.inat@hotmail.fr

**Abstract :** *The flow velocity above large scale roughness is investigated for low and steep slope between 0 and 4 %. The experiments were conducted in the laboratory of Fluid Mechanics Institute of Toulouse -IMFT. For the velocity measurement, the channel is equipped with a fast camera and a lightening system. The originality of the study lies in the application of a particle tracking technique (Particle Tracking Velocimetry). It is a non-intrusive measurement technique to measure instantaneous velocity in two-dimensional fields in stationary and unsteady flows. Analysis of the results is performed by processing images taken by the camera using a developed detection algorithm. A logarithmic distribution has been found for the velocity profiles which are influenced by roughness and slope. The obtained results show a depression of the maximum speed below the free surface. This behavior indicates a delay of the flow in the vicinity of the free surface and this is a direct consequence of the secondary flows presence in these areas.*

**Keywords—** *Free Surface Flow, Large scale Roughness, Experiments, Channel, Particle Tracking Velocimetry.*

## I. Introduction

The free surface flows in natural and urban environments, usually occur with inhomogeneous boundary conditions because of the distribution of the roughness of the bottom, fixed or mobile, and/or the large deformations of the free surface in particular for shallow currents against the bottom irregularities.

In flows under load or with free surface in rectilinear channels, the variations of the wall roughness are the source of secondary flows generated by the anisotropy of the turbulence and transverse variations of wall friction.

In open channel flows, the anisotropy of turbulence produced by the damping of vertical fluctuations of velocity under the free surface have an important role and it is responsible for significant differences between flows in load and flows with free surface.

In this context, an experimental study was conducted in the laboratory of Fluid Mechanics Institute of Toulouse "IMFT". In this study, only homogeneous bed roughness is considered because it is a first step to characterize the hydraulic resistance

and turbulent properties for large scale roughness as boulder or vegetation. The originality of our work is the application of a PTV Particle tracking technique (Particle Tracking Velocimetry).

One major advantage of this technique is that the flow field structures can be examined at a prescribed instant of time in total. However, this measurement method has also some limitations such as, this technique lies in its ability to gather large amounts of flow field information in the form of image data and usually re-quires the analysis of a large number of images (Adamczyk & Rimai, 1988).

By means of a fast camera, we determined the longitudinal evolution of the fields of average velocity, and Reynolds stress ( $\overline{u'w'}$ ).

The measurement technique is firstly described and then applied to flow over rough bed with a steep slope and a large-scale roughness (Pagliara and al., 2008). A large number of experimental correlations are available for this kind of flow (Rice and al., 1998) but the velocity measurements are rarely completed. This can be linked to the difficulty of using an intrusive probe in flow with low water depth in laboratory flume.

Several studies have been conducted to investigate the flow over rough bottom. We can quote some of these works: Chouaib Labiod (2005) realized experiments with a mode of setting up of the bars on the bottom of channel. The strips have a length equal to the channel width and thus the roughness of the bottom is homogeneous; Emma Florens (2010) also realized experiments with macro roughness on the channel bottom; Zaouali Sahbi (2008) studied the structure and the modeling of free surface flows in channels with inhomogeneous roughness.

## II. Experimental Design

### Description of the open channel

The experimental device (Figure. 1.) is composed of a rectangular channel made of glass, open pit having length of 4 m, a height equal to 0.8 m and a width of  $B=0.4$  m. The slope of the channel being adjustable, and varies between 0 and 6%. Circulation loop (stable) water is provided by an electric pump

providing a maximum throughput of 20 l/s. This pump delivers water through a pipe from a downstream tank from the channel to another upstream.

The control of the water level is done using a valve downstream of the channel and the flow control is done with a guillotine valve. Flow rates, Q, were measured using electromagnetic flow meters KRHONE with an accuracy of 0.5%.



Figure.1. the Channel and the annexes

This device allows reproducing a large range of natural river flows as shown in the table 1 and 2.

Table.1. experimental Froude number

	5 l/s	10 l/s	15 l/s	20 l/s
0 %	0.50	0.57	0.62	0.65
1 %	0.67	0.80	0.84	0.90
2 %	1.08	1.06	1.29	1.31
3 %	1.14	1.56	1.54	-
4 %	1.53	1.58	1.75	-

Table.2. experimental relative water depth h/k<sub>s</sub>

	5 l/s	10 l/s	15 l/s	20 l/s
0 %	5.64	8.23	10.29	12.02
1 %	4.68	6.59	8.36	9.68
2 %	3.40	5.47	6.30	7.53
3 %	3.28	4.22	5.58	-
4 %	2.70	4.20	5.14	-

### Roughness Configuration

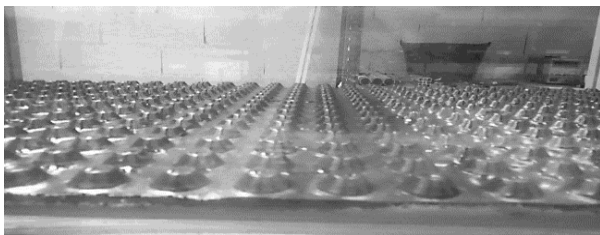
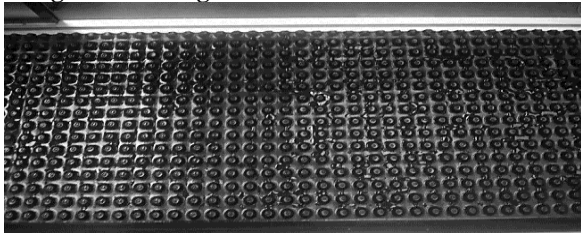


Figure.2. the channel bottom roughness

On the bed, initially smooth, we stuck in the longitudinal direction of the flow equidistant roughness lurking distributed throughout the channel (Figure 2.).

Thus, we achieve a high uniform roughness background, object of our study (Figure 3.). The roughness density  $\lambda$  is about 24 % if we consider the averaged diameter (D) of 14 mm. The transversal ( $a_x$ ) and longitudinal ( $a_y$ ) distance between two rough elements allows defining the density as follows:

$$\lambda = \frac{\pi D^2 / 4}{a_x a_y} \quad (1)$$

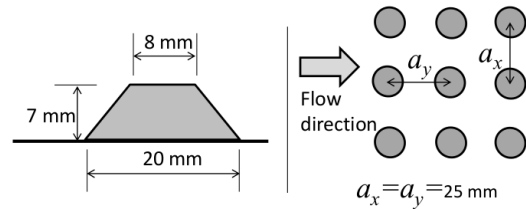


Figure.3. geometrical description of the roughness used over the bed.

### Measurement Technology: PTV (Particle Tracking Velocimetry)

In this study, the measuring means developed and used corresponding to a particle tracking technique (Particle Tracking Velocimetry) using a fast camera (Figure 4.). This is a non-intrusive measurement technique for measuring two-dimensional fields of instantaneous velocities in unsteady and steady flows. It consists in inoculating the flow study using reflective particles, having a diameter about 2 mm and the same density as the fluid, which will be illuminated with an illumination plane (Cassan & al, 2014).

A fast camera (1024 \* 1280 pixels) allows you to view the free surface of a pattern by ombroscopy, placed face a LED lighting system to differentiate the air from the water. The acquired image sequence sets the gray scale particles which, after treatment, will have access to the two components of the velocity vector in the plan.

Compared to other measuring methods, the PTV is an effective way to access instantly to different spatial scales of a turbulent flow in the same plane. Indeed, while the LDV, for example, requires a lot of careful movement of the equipment to obtain a high spatial resolution in a measuring plane in question, PTV provides, in the same plane, the information at the same instant in each point of space (Adamczyk & Rimai (1988)).

A series of 5000 images is taken for each flow rate. The averaged time value is determined by calculating the averaged signal for each pixel. This enabled us to calculate a mean for the water depth in the transverse direction. The free surface is identified by the minimum signal. A mean water depth of the pattern is then derived by integrating the free surface in the longitudinal direction. The slopes of the channel tested are: S = 0, 1, 2, 3 and 4%. The flow rates for each slope are respectively: Q = 5, 10, and 15 and 20 l/s.

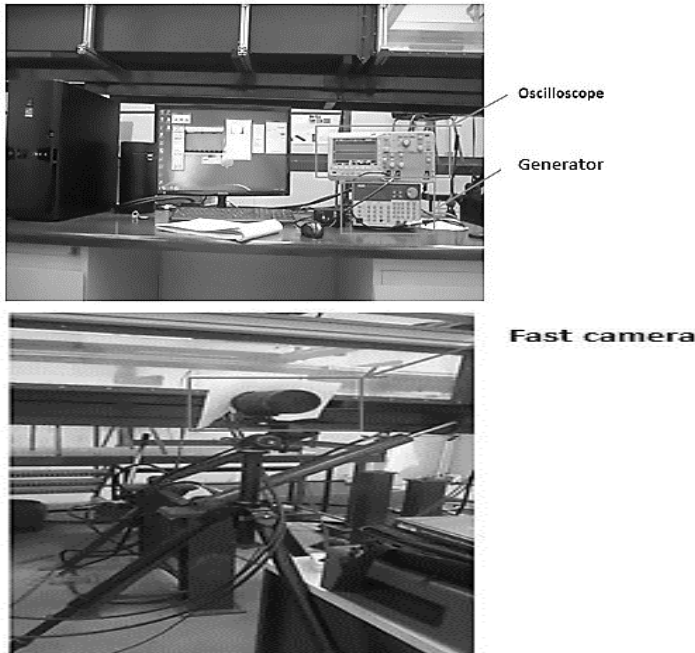


Figure 4. the PTV equipment's in the laboratory of IMFT

By determining the displacement of a particle between two consecutive images, we can measure the velocity. Analysis is performed on a large number of particle detection. By grouping the measures in areas of 30 pixels, we obtain a cartography of the averaged transversely velocity field (Figure 5.).

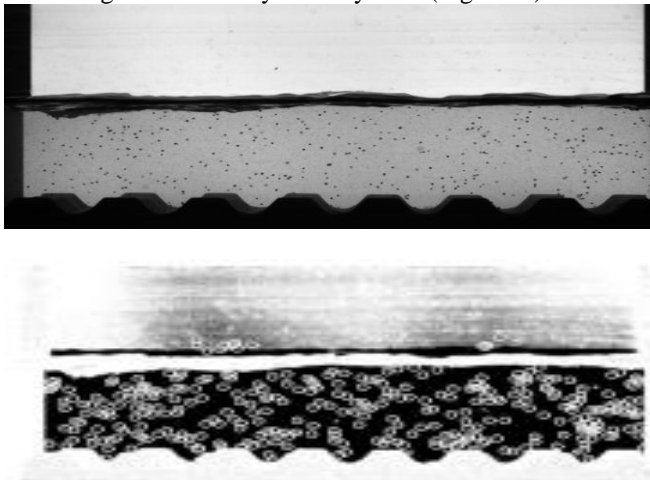


Figure 5. Experimental picture (top) for  $S = 1\%$ ,  $Q = 10l/s$  and particles detected in white circle (bottom).

It is observed that wrong detection can occurs. To delete these wrong values, the measurement distribution is calculated by 100 equal's steps. If the number of sample is lower than 20 % of the samples maximum number, the data is deleted. This method allows to keeps values if 2 peaks exists in the distribution. Moreover, using a standard deviation filter would oblige to make assumption on the turbulence properties (Figure 6.).

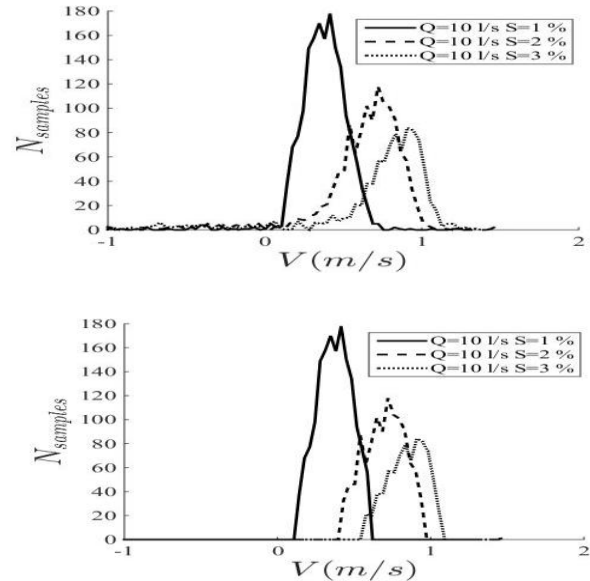


Figure 6. Velocity distribution for a cell at the center of the picture at 2 cm from the bottom before filtering (top) and after filtering (bottom)

The statistical convergence is also checked by plotting values as a function of samples number used. It could be shown (Figure 7.) that the measured values become insensitive to the sample number if they are superior to 700 which is the case for the present measurements. The method also needs a spatial homogeneity of particle density which is obtained by a strong turbulent mixture due to a closed circuit and flow over pumping system.

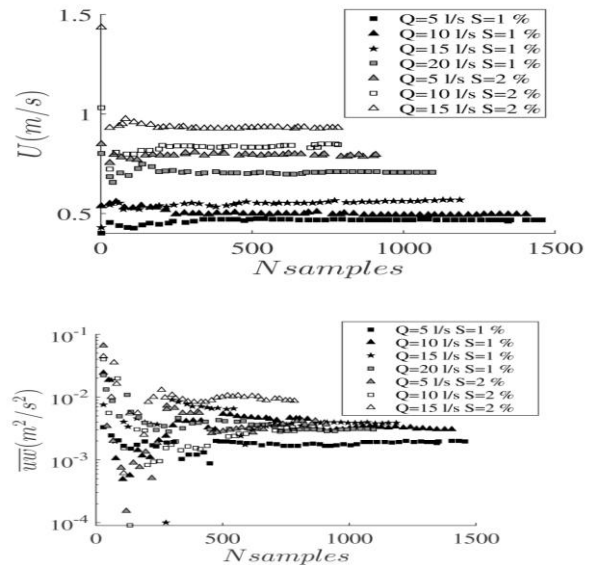


Figure 7. Statistical convergence of velocity (Top) and Reynolds stress (Bottom) at the center of the picture at 2 cm from the bottom.

The Stokes number is a dimensionless number used in fluid dynamics to study the behavior of a particle in a fluid. It represents the ratio between the kinetic energy of the particle to the energy dissipated by friction with the fluid. It is defined as follows:



$$S_t = \frac{\rho_p^2 D^2 P U}{\mu L_c} \quad (2)$$

Where:

$\rho_p$ : Density of the particle (1 kg / m<sup>3</sup>)

$d_p$ : Characteristic length of the particle (0.0008 m)

U: Cinematic fluid velocity

$\mu$ : Dynamic viscosity of the fluid (10 kg/ m.s)

$L_c$ : Characteristic length (m)

This number is used to determine the behavior of a particle in a fluid encountered an obstacle and in particular whether the particle will circumvent the obstacle (if  $S_t < 1$ ) by following the movement of fluid or if it will percolate the obstacle (if  $S_t > 1$ ). In our case, the Stokes numbers are given in the table 3.

**Table.3. the stokes number for the different runs**

	S= 1 %	S=2 %
Q <sub>1</sub> (5 l/s)	2 10 <sup>-7</sup>	3 10 <sup>-7</sup>
Q <sub>2</sub> (10 l/s)	3 10 <sup>-7</sup>	5 10 <sup>-7</sup>
Q <sub>3</sub> (15 l/s)	4 10 <sup>-7</sup>	6 10 <sup>-7</sup>

The Stokes number is small, so it is in a case where the particles follow the water flow.

### III. Experimental results

Several tests were made to validate the measurement methodology. We worked with different frame frequency and different numbers of images per sequence (10000 and 5000 images). It appears that this is the maximum frequency given by the frequency generator which gives the most accurate results. Secondly, we choose to work with 5000 images per sequence because with 10000 images the recording and processing are slower and the accuracy is not increased by supplementary images.

In the following results, therefore we kept a number of image 5000 im / Seq, and we worked with the maximum frequency of 360 Hz.

#### Bed friction coefficient

The spatially averaged water depth is given in the table 2. It is obtained by finding the minimum of the signal above roughness for the average picture of each experimental series. A longitudinal average is made numerically by averaging all cells (30\*30 pixels) at a given vertical coordinate. The shear velocity is also computed thanks to the momentum balance above the roughness:

$$u_* = \sqrt{gs(h - k_s)} \quad (3)$$

Firstly, the total conveyance of the channel is analyzed. To this end, the stage-discharge relationship is expressed in term of manning coefficient. A special attention is paid to the definition of the water depth for this kind of flow. Indeed, the flow within

the rough layer can be significant since the macro roughness are non-contiguous (Figure 8.). The friction factor is deduced thanks to the following formula:

$$\frac{n}{h_{ref}^{1/6}} = \frac{B h_{ref}^{3/2} \sqrt{S}}{Q} \quad (4)$$

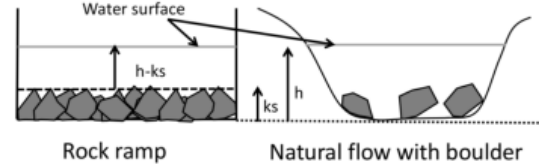


**Figure.8. Schematic view of flow area for 2 kind of steep slope with large roughness**

Where  $h_{ref}$  is the water depth considered (h or h- $k_s$ )

To get only the friction due to the roughness, the experimental value of n is corrected to the friction on the glass sidewall as proposed by Pagliara et al. (2008). For determination of the shear velocity when S= 0%, the Limerinos correlation (Limerinos, 1970) is used because it was validated for the other slope as explained below. The measurement of the free surface slope is not taken into account because the variation of the surface position differs from around 10 pixels which do not provide a sufficiently accurate value (Figure 9.).

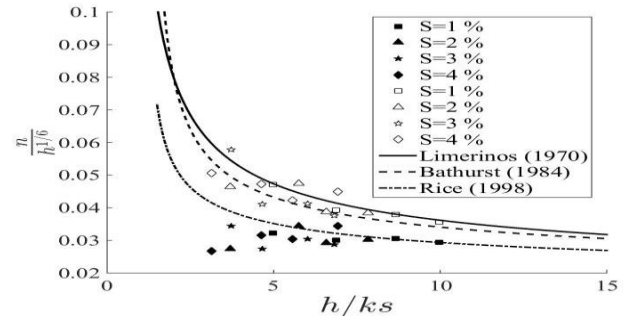


**Figure.9. Friction coefficients compared to formula from literature. Open signs correspond to calculus with  $h_{ref} = h$  and full signs to calculus with  $h_{ref} = h - k_s$**

The measurements are consistent with the experimental formula from literature. Both Limerinos (1970) and Bathurst (1984) consider  $y \approx h$  for natural flows whereas Rice et al. (1998) took into account the water depth above the roughness because the study is focused on contiguous rock ramps. Therefore, it better reproduces the experiments considering h- $k_s$ .

In fact, in general, for natural applications as steep rivers, the water depth is usually defined from the bottom because rocks have large dimension and the space between them are also important.

The diameter D should modify the friction coefficient since the drag force on the roughness is the main component of the total friction effect. But it is interesting to notice that the horizontal height  $k_s$  seems to be the pertinent length scale for the

empirical formula evens though the roughness used has very different sizes in the vertical and horizontal direction.

It is difficult to find a clear influence of the slope on the friction coefficient. The measurement at  $S=4\%$  must be taken carefully because the uncertainty is increased by the very low water depth.

### Vertical distribution of velocity and Reynolds stress

In this study, only the double spatially averaged profiles are presented. The transversal integration is obtained by the experimental method as explained before. The longitudinal integration is provided numerically by averaging the picture over 6 ax.

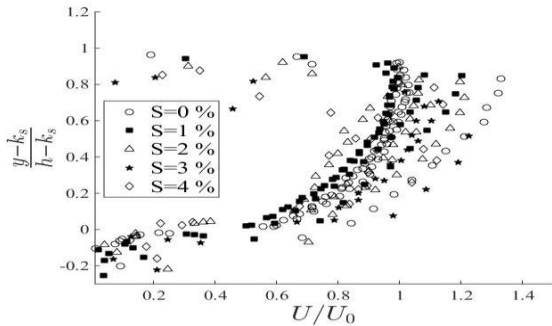


**Figure.10. Velocity profile obtained after averaging in the longitudinal direction**

The PTV method provides an estimation of the velocity which is important to quantify the part of the discharge flowing in the rough bed. The velocity of the bed is not strictly null because the cell resolution does not allow capturing the boundary layer over this very smooth surface.

A general overview of the velocity profile is given by the figure 10, where the velocity is divided by the bulk velocity  $U_0=Q/(Bh)$ . The velocity within the roughness is quite slower than those above.

The second general remark concerns the velocity profile near the surface. As the water surface oscillation in the 3 directions is hard to detect particles in this zone. Although the measurements near the surface are less accurate, it can be noticed that the increase of the slope tends to increase the maximal velocity compared to the bulk velocity. The position of the maximum moves downward and then modifies the distribution of the logarithmic law. Indeed, the following theoretical logarithmic distribution is assumed:

$$\frac{U}{u_*} = \frac{1}{\kappa} \ln \left( \frac{y-d}{z_0} \right) \quad (5)$$

The influence of hydraulic parameters ( $h/k_s$ ,  $Fr$ ,  $Re$ ) on the velocity profile are analyzed by determining the parameters  $d$  and  $z_0$  of the distribution (Eq.5) adjusted with the experimental data between. In this zone, the velocity profile is almost logarithmic as shown by the figure 11 where the solid line is given by the equation 5. No significant relationship was found between these parameters and the Froude or Reynolds number. The shear velocity is deduced from Eq. 3 and appears to be relevant to express the velocity profiles.

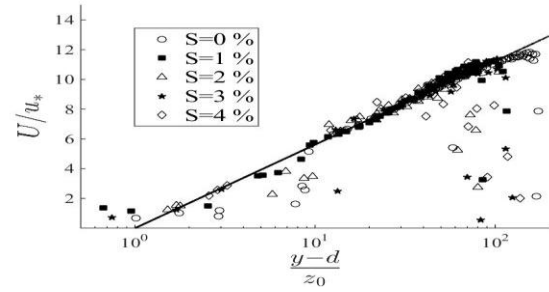


**Figure.11. Velocity profile obtained after averaging in the longitudinal direction and normalized by the shear velocity. The solid line is given by the equation 5.**

The measured  $d$  values which provide the better agreement with experiments is between 0,2 and 1 with an averaged value of 0.7. These values are consistent with the ones commonly observed (Defina and Bixio, 2005, Luhar et al. 2008).

In these experiments the rough density remains constant however  $z_0$  can also depend on the shear velocity and on the relative water depth ( $h/k_s$ ) (Cassan and Laurens. 2017; Defina and Bixio, 2005). For a rough bed, the value of  $z_0$  is usually taken equal to  $0.031 k_s$  which corresponds to a roughness function  $C(k_s u_* / \square) = 8.5$ . But on the figure 12., it can be noticed an increase of  $z_0/k_s$  as a function of  $h/k_s$ . Therefore, we emphasized the importance of considering flow around large macro roughness if the hydraulic roughness has to be known accurately. To model the evolution of  $z_0/k_s$ , it would be necessary to compute velocity inside the roughness which will be done in a future work.

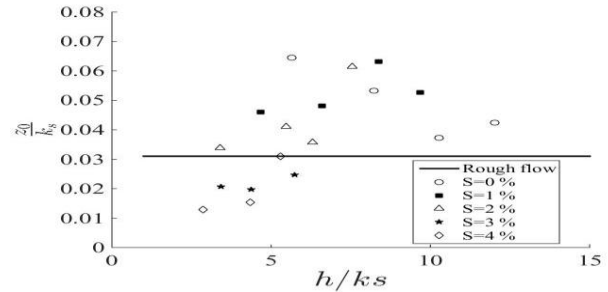


**Figure.12. Hydraulic roughness as a function of the relative water depth.**

### Turbulent distribution

The experimental method is a simple means to know the double spatially averaged value of  $u'w'$ , where  $u'$  and  $w'$  are the instantaneous velocity fluctuation in the longitudinal and vertical direction. The temporal averaged represents the Reynolds stress which is depicted on the figure 13.

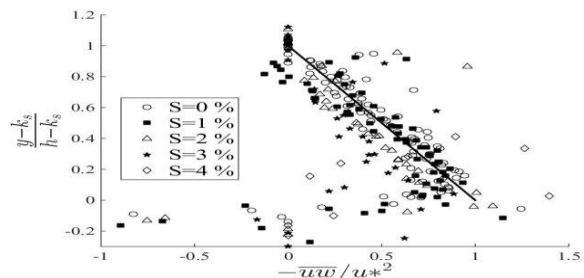


**Figure.13. Vertical distribution of Reynolds shear stress**

The solid line in the figure 13. represents the theoretical profile for turbulent shear within a boundary layer between  $k_s$  and  $h$ .

For all experiments, the linear vertical distribution is measured excepted for measurement near the surface. The experiments with  $S = 4\%$  also differs from the theoretical distribution but this issue can be linked to the very low water depth and free surface movement which disturb the particles detection.

The second important remark is the good accordance between the value of  $u^*$  deduced from the momentum balance and the

maximum value of the  $\overline{u'w'}$  ( $\overline{u'w'} = u_*^2$ ), corresponding to a possible second method of determining of  $u^*$ ; in fact, the shear velocity can be determined from the linear extrapolation of the

$$\frac{y - k_s}{h - k_s} = 0$$

profiles of the turbulent stress until the origin

Moreover, the maximum is located above the top of the roughness as already observed in the literature (Florens, 2013). Within the roughness, the distribution is non-linear due to the hidden part of the flow behind roughness.

Finally, the distribution of the turbulent kinetic energy ( $k$ ) is also depicted on figure 14. As the velocity is integrated laterally  $k$  is defined as follows:

$$k = \frac{1}{2}(\overline{u'^2} + \overline{w'^2}) \quad (5)$$

The ratio between  $k$  and  $u_*^2$  seems to be quite different as function of the slope and the Froude number. The steep slope shows a behavior which tends to the distribution for smooth bed since  $k/u_*^2 \approx 4$ .

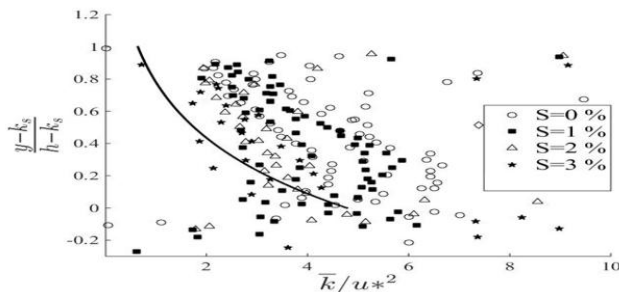


**Figure.14. Vertical distribution of turbulent kinetic energy. line represents the experimental correlation for smooth bed (Nezu and Nakagawa, 1993)**

Although for lower slope the Froude number is lower, the flow between rough elements seems to modify strongly the turbulent properties in the upper part of the roughness since the vertical distribution is almost uniform (Figure 14.). Let us note that for a given discharge, the Reynolds number is constant whatever the slope. As a consequence, it cannot explain the observed difference.

#### IV. Conclusion

Experiments in a laboratory experimental channel with a uniform roughness on the bottom were conducted. The technique of PTV has been developed and used for the determination and measurement of the velocity components and turbulent properties.

It should be noted that one advantage of the bottom roughness

is to slow the vertical velocity of the flow. Influence of the slope and the roughness on the velocity profiles were pointed out. In particular, the knowledge of  $u^*$  provides a good estimation of the discharge and turbulence even if the hydraulic roughness can differ from the classical rough bed value. In the results found we highlight the presence of a depression of the maximum velocity below the free surface. This behavior indicates a retardation of the flow near the free surface which is a consequence of the secondary flows presence in these areas.

Other experiments with vegetated bottoms will be performed in a larger channel at the National Agronomic Institute of Tunis (INAT), to determine the effect of vegetation on the flow characteristics.

#### Acknowledgement

This work is done at the Institute of Fluid Mechanics of Toulouse (IMFT), we dedicate the members of the HEGIE group for their help during the experiments.

#### References

- i. Adamczyk, A. A.; Rimai, L. 1989. 2-Dimensional particle tracking velocimetry (PTV): Technique and image processing algorithms. *Experiments in Fluids*, 6, 373-380.
- ii. Cassan, L. Hydraulic resistance of emergent macro-roughness at large Froude numbers. 2014. *Design of nature-like fish passes. Journal of Hydraulic Engineering*, 140.
- iii. Cassan, L.; Laurens P. 2017. *Design of emergent and submerged rock-ramp fish passes. Knowledge Management of Aquatic Ecosystem, to be published.*
- iv. Defina, A. ; Bixio, A. 2005. Mean flow and turbulence in vegetated open channel flow. *Water resources research* , 41, 1-12.
- v. Chouaib, L. *Écoulement à surface libre sur fond de rugosité inhomogène.* 2005. PhD thesis. Université de Toulouse, France, 39-56.
- vi. Florens, E. *Couche limite turbulente dans les écoulements à surface libre : Etude expérimentale d'effets de macro rugosités.* 2010. PhD thesis. Université de Toulouse, France, 110-130.
- vii. Florens, E. ; Eiff, O., Moulin, F. Defining the roughness sub layer and its turbulence statistics. 2013. *Exp. Fluids*, 54, 1-15.
- viii. Luhar, M. ; Rominger, J., Nepf, H. Interaction between flow, transport and vegetation spatial structure. 2008. *Environ Fluid Mech*, 8, 423-439.
- ix. Nezu, I.; Nakagawa, H. 1993. *Turbulence in Open-Channel Flows*, A.A. Balkema, Netherlands.
- x. Pagliara, S.; Das, R.; Carnacina, I. Flow resistance in large-scale roughness conditions. 2008. *Canadian Journal of Civil Engineering*, 35, 1285-1293.
- xi. Rice, C.; Kadavy, K.; Robinson, K. Roughness of loose rock riprap on steep slopes. 1989. *Journal of Hydraulic Engineering*, 124, 179-185.
- xii. Talbi, S.H.; Soualmia, A.; Cassan, L.; Masbernat, L. *Study of Free Surface Flows in Rectangular Channel Over Rough Beds.* 2016 *Journal of Applied fluid mechanics*, 9.
- xiii. Zaouali, S. *Structure et modélisation d'écoulements à surface libre dans des canaux de rugosité inhomogène.* 2008. PhD thesis. Université de Toulouse, France, 83-96.